Soft Matter

Dynamics of Lubricous, Concentrated PMMA Brush Layers Studied by Surface Forces and Resonance Shear Measurements

Journal:	*Soft Matter*
Manuscript ID	SM-ART-06-2019-001133.R1
Article Type:	Paper
Date Submitted by the Author:	12-Aug-2019
Complete List of Authors:	Mizukami, Masashi; Tohoku Daigaku, Institute of Multidisciplinary Research for Advanced Materials Gen, Masao; Tohoku University, Institute of Multidisciplinary Research for Advanced Materials Hsu, Shu-Yao; Kyoto University, Institute for Chemical Research Tsujii, Yoshinobu; Kyoto University, Institute for Chemical Research Kurihara, Kazue; Tohoku University, Institute of Multidisciplinary Research for Advanced Materials

Dynamics of Lubricous, Concentrated PMMA Brush Layers Studied by Surface Forces and Resonance Shear Measurements

*Masashi Mizukami[a], Masao Gen[1], Shu-Yao Hsu[b], Yoshinobu Tsujii[b] and Kazue Kurihara[a,c]**

[a] Institute of Multidisciplinary Research for Advanced Materials, Tohoku University, Sendai, 980-8577, Japan

[b] Institute for Chemical Research, Kyoto University, Uji, Kyoto 611-0011, Japan

[c] New Industry Creation Hatchery Center, Tohoku University,Sendai,Sendai, Sendai, 980-8599, Japan

We employed surface forces and resonance shear measurement (RSM) for studying the structure and properties of typical concentrated polymer brushes (CPBs) of poly(methylmethacrylate) (PMMA) in toluene, which are known to show a very low friction. The surface forces measured between the silica surfaces bearing PMMA brush layers showed a steric repulsive force at distance between silica surfaces less than ca. 1050 nm (D_{onset}). Upon retraction after compression of the PMMA brush layers, no adhesive force was observed. This indicated that the interpenetration of

the polymer chain was not induced by the normal load. Based on the resonance shear measurement, the elastic (k_2) and damping (viscous) (b_2) parameters, which represent the dynamic properties, of the PMMA brush layers were obtained by analyzing the resonance curves. At distances below the D_{onset}, the b_2 value significantly increased and slightly decreased at the higher normal loads, and the k_2 value monotonically increased with the increasing load. These k_2 and b_2 values were greater than those obtained for a PMMA brush layer and a bare silica surface (PMMA-silica). This indicated that the mobility of polymer chains for the PMMA-PMMA brush layers was more suppressed compared to that for the PMMA-silica, due to the interpenetration of the polymer chains. The interpenetration of polymer chains, commonly not observed for CPBs, could be most probably induced by the application of both the normal load and oscillating shear motion. With the increasing shear amplitude on the compressed PMMA-PMMA brushes (at L = 0.84, 1.34 and 4.28 mN), the b_2 value first increased then decreased whilst the k_2 value monotonically decreased. These tendencies can be explained by the change from the sticking condition due to interpenetration (high k_2), small sliding under interpenetration (increase in b_2, decrease in k_2), and then smooth sliding by pulling out of interpenetrated polymer chains (decrease in b_2 and k_2). The obtained results indicated that the operating conditions are quite important for using polymer brush layers as tribological materials because they can exhibit both a high and low friction depending on the conditions such as the load and shear amplitude.

1 INTRODUCTION

Polymers that are sufficiently densely adsorbed (or grafted) onto a surface (or interface) are called polymer brushes, which stretch away from the surface in their good solvents. They have received significant attention as functional surfaces in a number of scientific and technological areas. These includes colloid stabilization and destabilization,[1, 2] adhesion,[3] rheology, anti-fouling coatings,[4] and tribology.[5-7] One of the most effective applications of polymer brushes is lubrication. For lubrication in an aqueous solution, even semi-dilute polymer brushes with densities (σ) below 0.1 chains/nm^2 reduced the coefficient of friction to the order of 10^{-4}. Examples of such polymer brushes include charged polymer brushes (σ = 0.063 chains/nm^2)[6] and polyzwitterionic brushes (σ = 0.082 chains/nm^2).[8]

Over the past two decades, surface initiated living radical polymerization (LRP) was successfully applied to prepare well-defined polymer brushes with remarkably high graft densities (concentrated polymer brushes (CPB), i.e., σ > ca. 0.4 chains/nm^2).[9-14] Recently, by using the CPBs, a very low coefficient of friction (μ) was reported even in a nonaqueous solution in which the electrostatic repulsion could not be effective. For example, the coefficient μ of 5 x 10^{-4} was observed between the poly(methyl methacrylate) (PMMA) brush layers (σ = 0.53 chains/nm^2) swollen in toluene using colloidal probe atomic force microscopy (AFM).[15, 16] This low friction was ascribed to opposed CPBs hardly mixing with each other due to their significant osmotic and elastic interactions.[15] However, a recent simulation study indicated the interpenetration of polymer chains on opposed surfaces might have critical effects on friction depending on the conditions such as load (pressure), shear, swelling.[16-18] Experimentally, however, the interlayer mixing has only been studied under very limited conditions. Employing opposed cross-linked polymer brushes, a different lubrication behavior from non-cross linked ones is observed and

interpreted by the effect of different interlayer mixing.[18] Employing the polymer brush with cyclic structures[19] or asymmetric polymer brushes layers which are immiscible[20], significantly reduced friction forces compared with those for linear polymer brushes are observed and interpreted by the suppression of the interlayer mixing. Although the graft densities of polymer chains in these reports were lower than that for CPBs (0.4 chains/nm^2), these studies indicate that the interlayer mixing of polymer chains could have significant effect on the friction. In order to apply CPBs for lubrication, especially under the condition of so-called boundary lubrication (high load and slow shear velocity), the understanding of the structure and properties including the mixing and the dynamics of CPBs under load (L) and shear, and optimizing their design for the required use of CPBs based on it are essential.

The most useful techniques to provide a molecular level insight into the CPBs and their dynamics are the surface forces measurement and resonance shear measurement (RSM) using a surface forces apparatus (SFA). SFA can measure the interaction forces (normal force, F, which is equal to the applied normal load (L) to the surface) between two cylindrical surfaces (curvature radius R = 20 mm) in crossed geometry as a function of the surface separation distance (D) at the distance resolution of 0.1 nm and the force (load) resolution of 10 nN. Thus, the SFA can evaluate the polymer brush thickness as a function of the normal load (L). In addition, resonance shear measurement (RSM), which we developed based on SFA, can analyze the tribological properties by applying an oscillation parallel to the surfaces and measure the shear response. The reason which prevented application of these techniques for CPBs is the availability of suitable substrates. Commonly, thin mica or silica sheet with a deposited silver layer glued on a half-cylindrical silica disc was used as a substrate for the surface forces and resonance shear measurements. The epoxy resin used for gluing easily dissolved into the organic solvents which are used for the preparation

of CPBs of PMMA by surface-initiated atom transfer radical polymerization (ATRP).[21] We have developed a method for the direct deposition of a smooth silica layer on the silica disc with an Au layer between them, and can avoid using a resin,[22] therefore, we are able to study CBSs under various conditions.

In this study, we employed the surface forces and resonance shear measurement (RSM) for studying the structure and dynamic properties of typical CPBs,[15] i.e., poly(methylmethacrylate) (PMMA) CPBs, in toluene, which show a very low friction. The surface forces measurement revealed that the PMMA brushes did not interpenetrate (mixing) by only applying a normal load. The interpenetration of the opposed PMMA brush layers was found to occur by applying a normal load as well as shear motion, thus resulting in a high friction force. We also found that the interpenetration of PMMA could be released and the friction force could be reduced by applying a shear motion with a higher driving amplitude and velocity.

2 EXPERIMENTAL SECTION

2.1 Materials

Half-cylindrical silica lenses with the curvature radius R = 20 mm (Sigma Koki Co., Ltd.) and cover glass plates (Matsunami Glass Ind., Ltd.) were used as the substrates. Just before deposition of the chromium layer, these substrates were cleaned using acetone in an ultrasonic bath for 5 min, rinsed with pure water, cleaned in piranha solution (sulfuric acid : hydrogen peroxide = 3 : 1) for 30 min, then dried under vacuum.

Methyl methacrylate (MMA, 99%, Nacalai Tesque, Japan) was passed through a column of basic alumina to remove the inhibitors. Cu(I)Cl (99.9%, Wako Pure Chemical, Japan), ethyl 2-bromoisobutylate (EBIB, 99%, Wako), 4,40 -dinonyl-2,20 -bipyridine (dNbipy, 97%, Sigma-

Aldrich Co., USA), and hexamethyldisilazane (HMDS, Tokyo Chemical Industry Co., Ltd., Japan) were used as received. (2-Bromo-2-methyl)propionyloxyhexyltriethoxysilane (BHE) was prepared as previously reported.[23] All other reagents were used as received from commercial sources.

2.2 Preparation of Polymer Brushes on Silica for RSM.

The silica substrates were directly deposited on the silica discs by the RF sputtering technique as previously reported,[22] and used for the preparing polymer brushes in toluene. Briefly, a chromium layer of 5 nm, then a gold layer of 41 nm in thickness were deposited on the silica discs (pressure < 10^{-3} Pa, deposition rate 0.007–0.008 nm/s, room temperature) by a vacuum deposition technique (VPC-250F, ULVAC KIKO, Inc.). Silica layers of ca. 2 μm thick were then deposited (rf power 200 W, pressure 0.5 Pa, deposition rate ca. 0.5 nm/s) on a Au/Cr/silica disc using the rf magnetron sputtering system (SPV2-TMP-T1-RF1/R, Toei Scientific Industrial Co., Ltd.), then annealed at 450 ˚C for 2 hours.

Well-defined CPBs of PMMA were prepared on these silica surfaces by surface-initiated atom transfer radical polymerization (SI-ATRP), as previously reported (Fig. 1). Briefly, the silica layer deposited by sputtering on the Au/silica disc (silica/Au/silica disc) was immersed in a toluene solution of BPE (1 wt%) for 24 h at 120–130 ˚C, then rinsed with toluene and stored in toluene. Subsequently, the BPE-immobilized silica/Au/silica disc was immersed in a degassed MMA and anisole mixture (50 : 50 w/w) containing EBIB (0.086 mM), Cu(I)Cl (0.86 mM), Cu(II)Cl (0.017 mM) and dNbipy (1.92 mM), sealed under an argon atmosphere in a Schlenk flask, and heated at 60 ˚C for 6 h. EBIB was added as a free initiator not only to control the polymerization but also to yield free polymers which is a good measure of the molecular weights of graft polymers (see below).[23, 24] After polymerization, the solution was subjected to gel permeation chromatographic

(GPC) measurements to determine the molecular weights of the free polymer and monomer conversions. The PMMA-grafted silica/Au/silica disc was copiously rinsed, then washed by ultrasonication in $CHCl_3$ to remove the physisorbed free polymers and impurities. The dry thickness, L_D, of the PMMA-brush layer was determined by ellipsometry (MIZOJIRI- OPTICAL, DHA-XA/S3-T). Table 1 lists the characteristics of the CPBs of PMMA studied in this paper. The number-average molecular weight, M_n, and the polydispersity index, M_w/M_n, are those of the free polymer analyzed by GPC calibrated with PMMA standards. It is reasonable to assume that these values should well approximate those of the graft chains.[23, 24] The graft density σ was calculated from M_n, L_D, the bulk density of a PMMA film ρ (=1.19 g/cm^3),[25] and the Avogadro constant N_A, using $\sigma = \rho L_D N_A / M_n$.

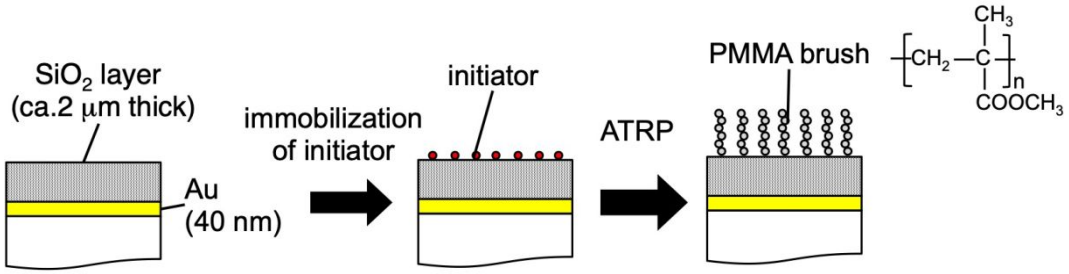

Fig. 1 Preparation of PMMA brush layer on silica surface by atom transfer radical polymerization (ATRP).

Table 1 Molecular characteristics of PMMA brushes prepared on silica surfaces.

Substrate	M_n	M_w	M_w/M_n	Graft density, σ (chains/nm^2)	Dry thickness, L_D (nm)
1	110100	129000	1.17	0.76	116.9
2	109600	128700	1.18	0.89	135.4

2.3 Surface Forces and Resonance Shear Measurement (RSM).

The surface forces and resonance shear measurements were performed to study the opposed PMMA brush layers as well as a PMMA brush layer and a sputtered silica surface immersed in toluene using RSM-1 (Advance-riko Inc.) (see Fig.2). The surface separation distance (D') of which zero was defined as the dry contact of the PMMA layers was determined using the fringes of equal chromatic order (FECO).[26] The surface separation distance (D) between the silica surfaces was then obtained by adding the dry thicknesses (L_D, see Table 1) of two PMMA layers to the D' value ($D = D' + 2L_D$). The FECO fringe images during the measurement were recorded using a sCMOS camera (ANDOR Neo, Oxford Instruments) equipped with a monochrometer. The wavelengths of the fringes in the recorded images were determined using the Hg lamp emission line (green and yellow) as the references. The lower surface was supported by a double cantilever spring (spring constant k_N = ca. 200 N/m) and driven by a pulse motor. The interaction force F (normal load (L)) was obtained at a resolution of 10 nN by measuring the deflection of a spring (Δd) using Hook's law ($F = k_N \cdot \Delta d$). The PMMA brushes prepared on the silica surfaces were equilibrated for more than 16 hours in toluene before starting the forces measurement. The interaction force (F) (normal load (L)) vs surface separation distance (D) profiles were obtained at drive speeds of 8 nm/s and 0.5 nm/s. The obtained force (F) was normalized by the curvature radius (R) of surfaces according to the Derjaguin approximation ($F/R = 2\pi G_f$, G_f : interaction free energy between flat surfaces of unit area).[27] The temperature inside the apparatus measured by a platinum resistance thermometer was equilibrated at ca. 24 ˚C by irradiation of a white light used for FECO.

The resonance shear measurement system was composed of an upper unit (an upper surface connected to the piezo tube and hung by a pair of vertical leaf springs) and a lower unit (a lower

surface mounted on the horizontal leaf spring). The upper unit was laterally moved by applying a sinusoidal voltage ($U_{in}\sin\omega t$, $\omega = 2\pi f$ (f : frequency)). The amplitude of the input voltage (U_{in}) was changed from 1.0 to 50 V to investigate the effect of the shear amplitude and velocity on the properties of the PMMA brushes. The deflection of the vertical spring ($x_{spring} = X_{spring}\sin(\omega t + \varphi_{spring})$) was measured by a capacitance probe (Mircosense 4830, Japan ADE) as an output voltage ($U_{out}\sin(\omega t + \varphi_{spring})$). The output amplitude U_{out} and its phase shift (φ_{spring}) from the input voltage U_{in} were determined by a two phase lock-in amplifier (5610B, NF Corporation), then recorded by a computer via a data acquisition (DAQ) board (NI PCIe-6351, National Instruments). The displacement of the upper surface ($x_1 = X_1\sin(\omega t + \varphi_1)$) around the resonance peak frequency was proven to be equal to the deflection of the vertical spring ($x_{spring} = X_{spring}\sin(\omega t + \varphi_{spring})$) at around the peak frequency by directly measuring both displacements.[28] Thus, the displacement of the upper surface can be obtained from the capacitance probe ($x_1 = x_{spring} = C_{out}U_{out}\sin(\omega t + \varphi_{spring})$. The resonance curves ($U_{out}/U_{in}$ vs. ω) were obtained by scanning the frequency of the input voltage U_{in} using a homemade LabVIEW program. It showed the maximum intensity U_{out}/U_{in_res} at a resonance frequency ω_{res} of the oscillating unit. The property of the liquids confined between the upper and lower surfaces as well as the properties of the polymer brushes could be evaluated with a high sensitivity based on the peak intensity (U_{out}/U_{in_res}) and frequency (ω_{res}). As reference curves, without sample liquids between the surfaces, the resonance curves were measured when the surfaces were separated by air (AS) and when the mica sheets glued on the silica discs were directly in contact in air (MC). The AS and MC resonance curves corresponded to the condition of no friction and no sliding, respectively.

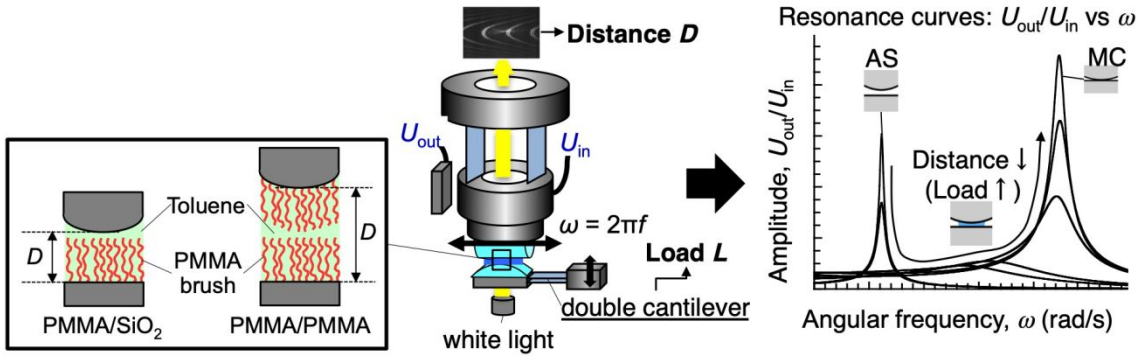

Fig. 2 A schematic drawing of resonance shear apparatus (left) and typical resonance curves at various surface separation distances D (load, L) (right).

2.4 Analysis of Resonance Shear Curves using Mechanical Model.

The resonance curves were analyzed by fitting with equation 1, which was derived from the mechanical model shown in Fig. 3.[29] The parameters of the upper unit (b_1, k_1, m_1) were determined by analyzing the AS resonance curve, and the parameters of the lower unit (b_3, k_3, m_2) were determined by analyzing the MC resonance curve using the determined upper unit parameters (b_1, k_1, m_1).

$$\frac{U_{out}}{U_{in}} = \frac{C}{\alpha}\sqrt{\frac{\left(K_2 - m_2\omega^2\right)^2 + \omega^2 B_2^2}{\left[\left(K_1 - m_1\omega^2\right)\left(K_2 - m_2\omega^2\right) - \omega^2 B_1 B_2 - k_2^2 + b_2^2\omega^2\right]^2 + \omega^2\left[\left(K_1 - m_1\omega^2\right)B_2 + \left(K_2 - m_2\omega^2\right)B_1 - 2k_2 b_2\right]^2}} \quad (1)$$

where, $B_1 = b_1/\alpha + b_2$, $B_2 = b_2 + b_3$, $K_1 = k_1/\alpha + k_2$, $K_2 = k_2 + k_3$, and C is an intensity parameter. The α value was fixed to 1, which was obtained by the direct measurement of x_1 (displacement of upper surface).[28]

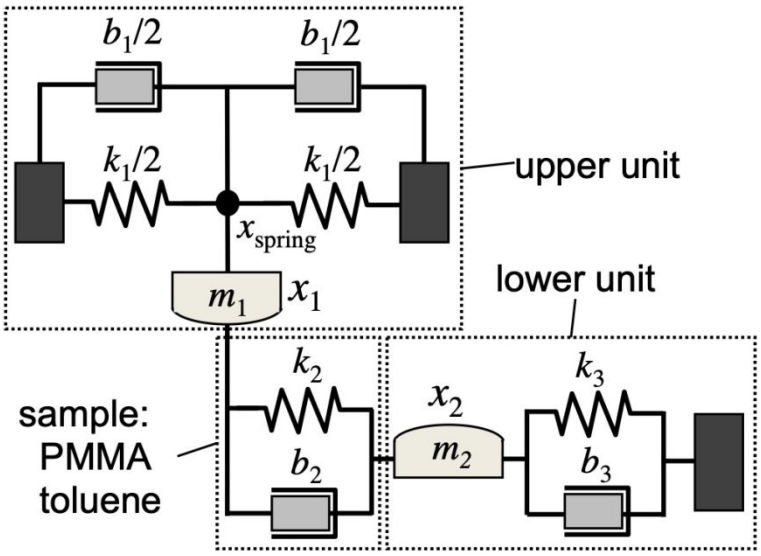

Fig. 3 A schematic illustration of a mechanical model used for analyzing the resonance curves. The parameters of b_1, b_2 and b_3 (Ns/m) are the viscous parameters of the upper unit, the sample, and the lower unit; and k_1, k_2, k_3 (N/m) are the elastic parameters (spring constants) of the upper unit, the sample (lubricant in this study), and the lower unit, respectively. The parameters of m_1 and m_2 are the effective masses of the upper and lower units, and x_1 and x_2 are the positions of the upper and lower surfaces, respectively. The x_{spirng} value is the deflection of the upper spring (k_1) directly measured by a capacitance probe and is equal to the x_1 value.

3 Results and Discussion

3.1 Surface Forces between PMMA Brush Layers.

In order to determine how the polymer brush layers stretch from the surface, the surface forces (F/R) between the PMMA brush layers was measured as a function of the surface separation distance (D) between the silica surfaces. Fig. 4 shows the surface forces measured with a constant driving speed (8 nm/s) of the lower surfaces on approach and retraction. On the first approach, a repulsive force significantly increased from a distance of D_{onset} = ca. 1050 nm, then monotonically increased with the decreasing D. The F/R value reached ca. 80 mN/m at 900 nm. The extended

thickness of the PMMA brush layer (L_{ext}) was estimated as half of D_{onset} ($L_{ext} = D_{onset}/2$ = ca. 530 nm). Thus, the swelling ratio ($L_{ext}/L_d - 1$) of the PMMA brush layer was estimated to be ca. 3.2, which was similar to the typical swelling ratio of concentrated polymer brushes.[15] Upon retraction, a large hysteresis in F/R vs D was observed, *i.e.*, the repulsive force very rapidly decreased with the increasing D. On the second approach, the repulsive force significantly increased from a distance of ca. 1000 nm, which was smaller than that of 1st approach indicating that the PMMA brush layer had not fully recovered to the original structure before the compression. The repulsive force on the 2nd retraction was almost the same as that of the 1st retraction. The surface forces observed on the 3rd approach and retraction were same as those of the 2nd. The structure changes should be in a steady state under this compression and decompression speed of 8 nm/s.

The surface forces profiles were measured with a slower driving speed of 0.5 nm/s to investigate the influence of the driving speed (see Fig. S1 in Supporting Information). For the first approach, the force profile steeply increased from a distance of D_{onset} = ca. 1050 nm, which was identical to the D_{onset} determined at the speed of 8 nm/s. The profile then monotonically increased with the decreasing D, identical to the speed of 8 nm/s till F/R = 3.4 mN/m, then showed a lower repulsive force compared to that obtained at the driving speed of 8 nm/s till a smaller distance. This means that the PMMA brush layers required a longer time to deform and deswell upon compression. Upon retraction, the much larger hysteresis was observed at 0.5 nm/s due to the brush layers being much more compressed than in the 8 nm/s case. This indicated that the relaxation of the polymer chain became much slower after the compression due to entanglement in the polymer chains. However, no adhesion was observed during the separation process of the PMMA brush layers. This indicated that no interpenetration of PMMA brushes was caused by compression.[30]

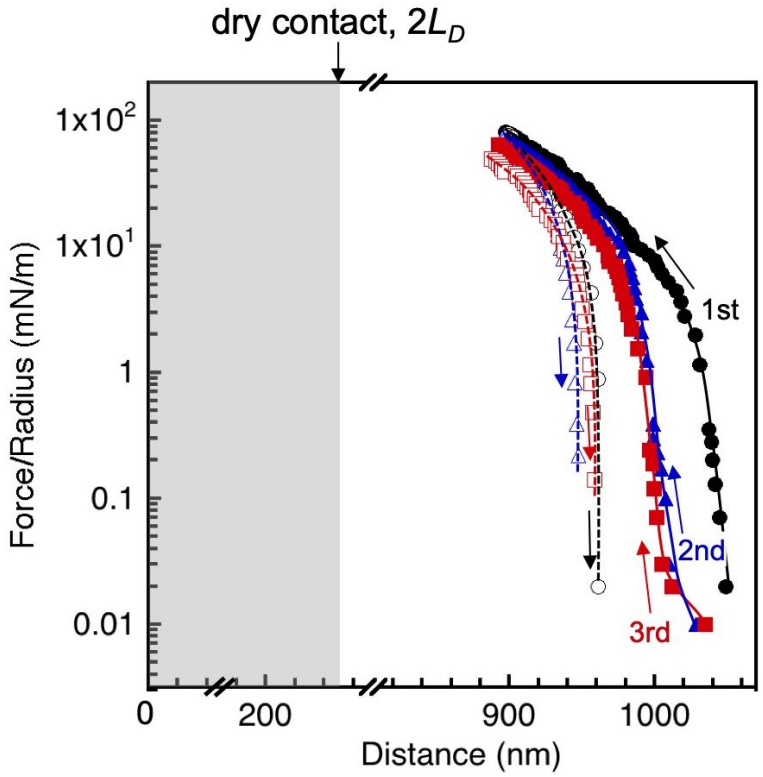

Fig. 4 Plots of force/radius (F/R) vs surface separation distance (D) of PMMA brush layers fabricated on silica surfaces. Here, the zero distance (D = 0 nm) was defined as the contact of the silica surfaces. The surface separation distance (D') of which zero was defined as the dry contact of the PMMA layers was determined using the fringes of equal chromatic order (FECO).[26] The surface separation distance (D) between the silica surfaces was then obtained by adding the dry thicknesses (L_D, see Table 1) of two PMMA layers to the D' value ($D = D' + 2L_D$). The approaching and retraction data are shown as filled and open symbols, respectively (1st:circle, 2nd:triangle, 3rd:square).

3.2 Resonance Shear Measurement on PMMA-PMMA Brush Layers.

In order to investigate the structure and properties of the PMMA-PMMA brush layers in toluene, the resonance shear measurement was performed by varying the surface separation distance and

normal load. Fig. 5 shows the resonance curves obtained for the PMMA-PMMA brush layers in toluene with the input voltage (U_{in}) of 1 V. The resonance peaks of AS (separated by air) and MC (mica contact) were observed at 198 rad/s and 351 rad/s, respectively. The MC peak frequency became higher than that of the AS peak because of the contribution of the lower horizontal spring to the resonance due to the strong adhesion between mica surfaces. At D = 1084 nm, which was greater than the onset of repulsive force (D_{onset} = ca.1050 nm shown in Fig. 4), the resonance peak frequency (ω_{res}) was located at a frequency almost the same as that of the AS peak (ω_{res_AS}), and its amplitude (U_{out}/U_{in_res}) decreased to 4.7 (87 % of the AS peak). At D = 1067 nm, which was slightly greater than D_{onset}, the U_{out}/U_{in_res} value slightly decreased to 3.9 (72 % of AS peak). This indicated that the oscillation energy dissipated due to the interaction between the edges of the PMMA-PMMA brush layers. At D = 1014 nm, which was smaller than D_{onset}, the ω_{res} shifted to a higher frequency (ca. 337 rad/s). This indicated the strong correlation of the opposed PMMA-PMMA brush layers. With the further decreasing D, the ω_{res} value shifted higher towards that of the MC peak, and the U_{out}/U_{in_res} value increased to 6.8 (90 % of MC peak) at D = 477 nm (normal load of 4.3 mN). This high peak amplitude (close to a no-slip condition of MC) indicated that the friction force became quite high[31] with the decreasing D (increasing load, L) unlike the previously reported very low friction coefficient obtained using a colloidal probe AFM.[15, 16] A possible cause of this high friction force could be the interpenetration of the PMMA chains between opposed layers induced by the oscillating shear motion under the applied normal load. The molecular weight (MW) of PMMA brush used in this study was much larger than the MW of entanglement in PMMA melt is 3 x 10^4,[32] and part of polymer chains might be entangled.

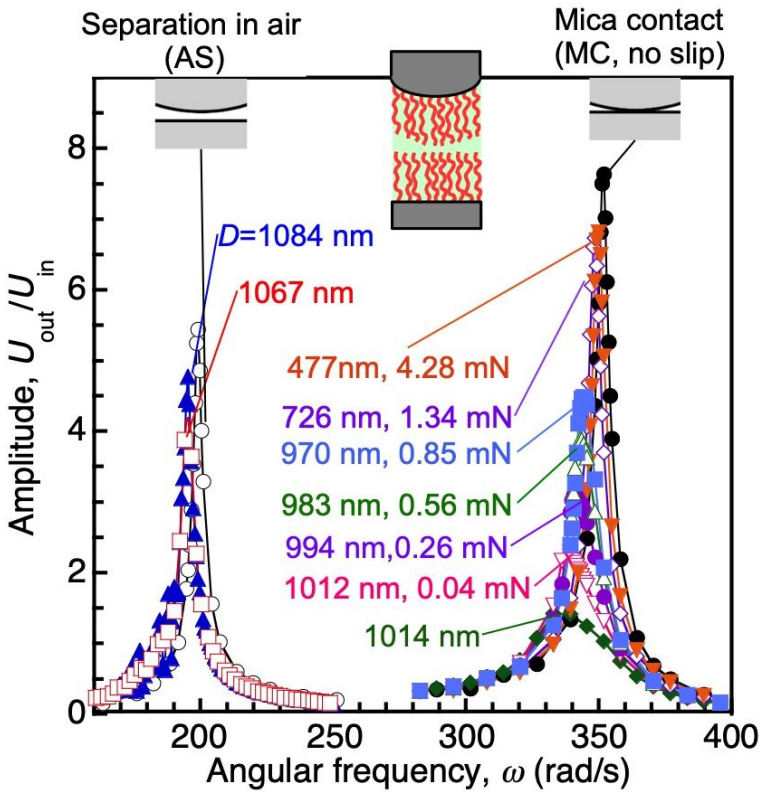

Fig. 5 Resonance shear curves between the PMMA-PMMA brush layers measured in toluene with a input voltage U_{in} of 1 V.

3.3 Resonance Shear Measurement on a PMMA Brush Layer and a Silica Surface.

The high friction force obtained by resonance shear measurement on the opposed PMMA-PMMA brush layers at the applied normal load (L) ≥ 0.04 mN indicated the interpenetration of the polymer chains. In order to examine the interpenetration of the opposed PMMA-PMMA chains under the applied load and shear, we performed the resonance shear measurement on a PMMA brush and a bare silica surface (PMMA brush-silica) in toluene in which no interpenetration could occur (Fig. 6). At D = 392 nm, at which the brush layer may start to touch the opposed silica surface, a weak peak was observed at 296 rad/s. With the decreasing D (increasing normal load), the peak amplitude (U_{out}/U_{in}) monotonically increased, and reached 5.1 (66 % of the MC peak) at D = 333 nm (at a normal load of 0.79 mN), which was slightly higher than the value (4.4) observed

for the PMMA-PMMA brush layers at the normal load of 0.85 mN. On the other hand, the peak frequency ω_{res} = 327 rad/s at D = 333 nm (normal load 0.79 mN) for the brush and silica was significantly lower than the ω_{res} = 350 rad/s observed for the PMMA-PMMA brush layers at a similar normal load (0.85 mN). The resonance peak frequency of the PMMA brush-silica system was always lower than the peak frequency of the PMMA-PMMA brushes as shown in Fig. 7. The lower peak frequency ω_{res} should correlate with the lower elastic parameter (k_2) of the oscillating unit, and could be intuitively related to the absence of chain interpenetration of the PMMA-silica system. To quantitatively compare the properties of the PMMA-PMMA brush layers as well as the PMMA brush-silica, the resonance curves were analyzed using equation 1 based on the mechanical model (Fig. 3).

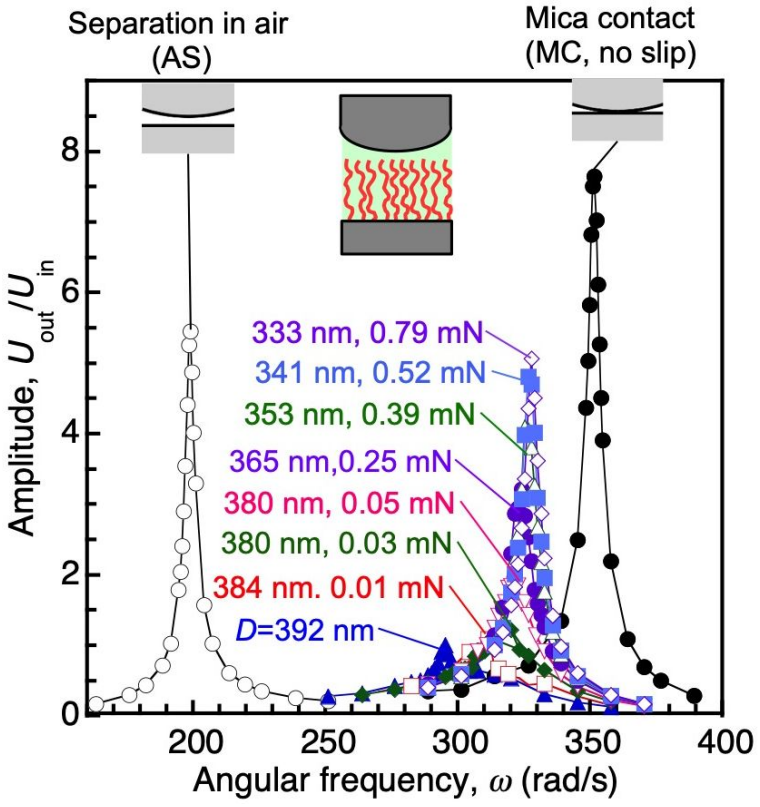

Fig. 6 Resonance shear curves between a PMMA brush-silica measured in toluene with a input voltage U_{in} of 1 V.

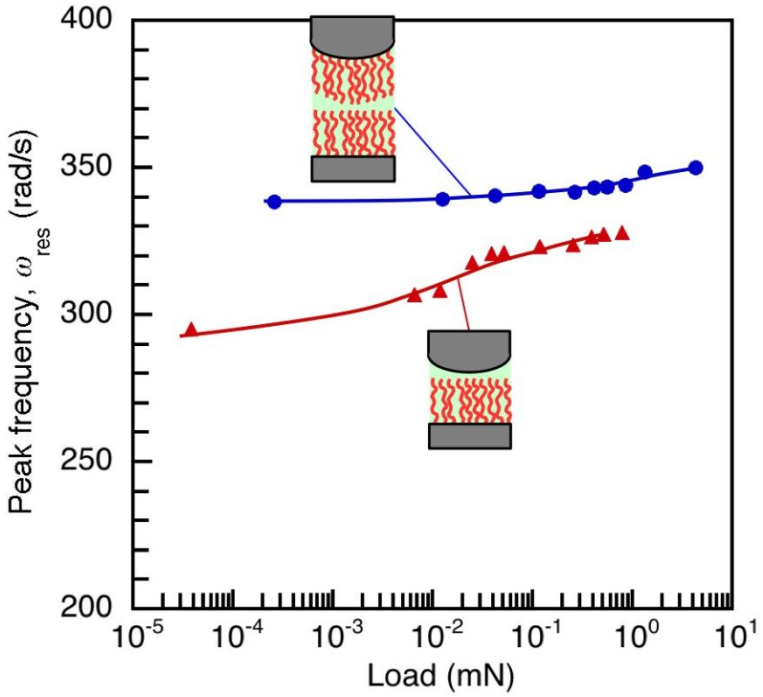

Fig. 7 Plots of the peak frequency (ω_{res}) vs the applied load (L) obtained for the PMMA-PMMA brush layers (blue filled circle) as well as for the PMMA brush-silica surface (red filled triangle).

3.4 Elastic and Damping Properties of PMMA-PMMA Blush Layers and PMMA Brush-Silica.

Fig. 8 (a) and (b) show the surface separation distance dependencies of the elastic (k_2) and damping (viscous) (b_2) parameters obtained by fitting the resonance curves for the PMMA-PMMA brush layers and the PMMA-silica using equation 1, respectively. We used the term "damping" for the b_2 parameter because we discuss the energy dissipation in the PMMA brush layers. The damping parameter (b_2) for the PMMA-PMMA increased about 4 orders of magnitude with the decreasing distance in the range of 1094 – 1030 nm (region (i) in Fig. 8(a)). The b_2 value then slightly decreased at distances in the range of 1030 – 480 nm (region (ii) in Fig. 8(a)). The damping parameter (b_2) for the PMMA brush-silica system increased with the decreasing distance in the range of 392 – 380 nm (region (i') in Fig. 8(a)), then decreased at the distances below 380

nm. The initial increase in b_2 value at greater distances of 1094 – 1067 nm for the PMMA-PMMA and of 392 – 380 nm for the PMMA-silica may due to the confinement effect on toluene previously observed for various liquids[31, 33-36] and/or the contact of terminal chains of polymer brushes for the former and polymer brush-silica for the latter. This, however, did not produce any detectable increase in the normal repulsion.

The elastic parameter (k_2) for the PMMA-PMMA layers was below the detection limit (< 0.1 N/m) in the distance range of 1094 – 1067 nm (region (i) in Fig. 8(b)), then drastically increased with the decreasing distance below 1030 nm, and reached 46000 N/m at D = 477 nm. In the case of a PMMA brush-silica, the k_2 value was 1860 N/m at D = 393 nm, increased with the decreasing distance, then reached 5300 N/m at D = 328 nm.

The damping (b_2) and elastic (k_2) values were also plotted versus the normal load (L) applied to decrease the distance (D) in Fig. 9 (a) and (b), respectively. In these plots, in order to focus on the properties of the polymer brushes, the changes in the b_2, k_2 and L values are shown for the distance range (ii) and (ii') in Fig. 8(a). Both the elastic (k_2) and damping (b_2) parameters of the PMMA-PMMA brush layers were higher than those of the PMMA brush-silica in the entire range of the applied load. These results supported the interpenetration of the polymer chains under the normal load and shear for the PMMA-PMMA brush layers. One may note that no adhesion was observed in the normal forces measurement (without oscillating shear) between the PMMA-PMMA brush layers, indicating no significant interpenetration occurred between the brush layers without applying shear to the layers. The osmotic pressure of polymer chains usually prevents the interpenetration of polymer brushes. This study demonstrated that the application of the oscillating shear between polymer brushes induced the interpenetration overwhelming the effect of osmotic pressure. However, the normal load dependencies of the elastic (k_2) and damping (b_2)

parameters could not be intuitively understood. The reason for this difficulty is that the shear amplitude between upper and lower surfaces changes depending on the k_2 and b_2 parameters in the RSM (see Fig. S3), which produces complicated changes in k_2 and b_2 vs L. Therefore, in order to understand how the properties and structure of the PMMA-PMMA brush layers depend on the conditions (normal load, shear amplitude, and shear velocity), we performed the RSM at various drive amplitudes by changing U_{in} from 1 to 50 V.

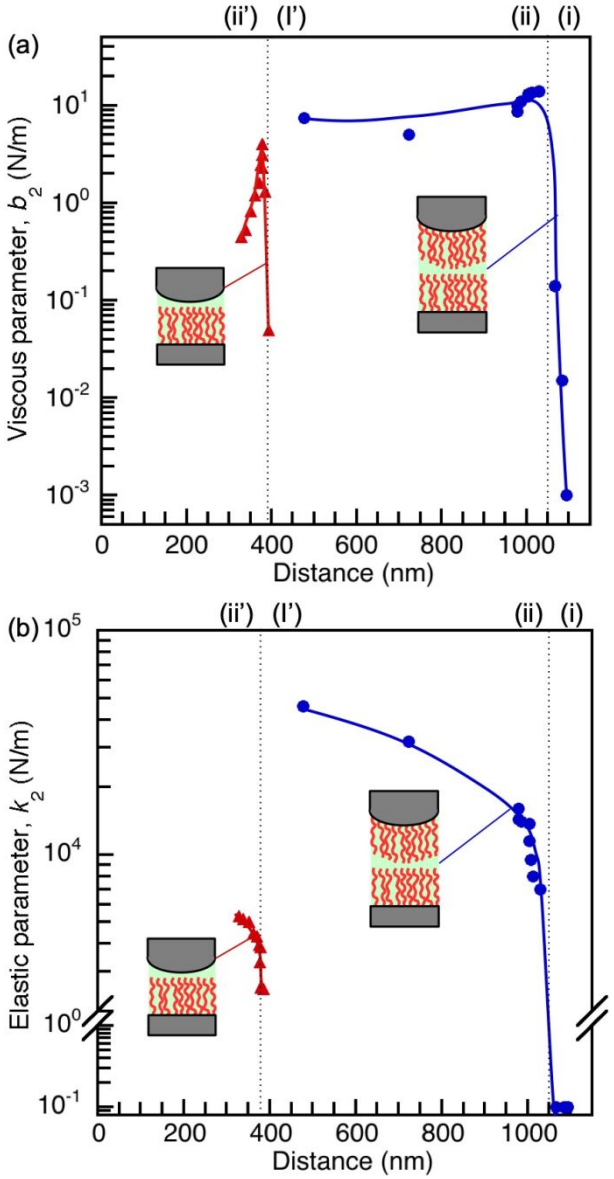

Fig. 8 (a) Plots of elastic (k_2) parameters vs surface separation distance (D) obtained for the PMMA-PMMA brush layers (blue filled circle) as well as for the PMMA brush-silica surface (red filled triangle). (b) Plots of viscous (b_2) parameters vs surface separation distance (D) obtained for PMMA-PMMA brush layers (blue filled circle) as well as for PMMA brush-silica surface (red filled triangle). The regions (i) and (ii) denote distance range where the PMMA brush layers are not in contact and are in contact, respectively. The regions (i') and (ii') denote distance ranges where the PMMA brush layer and the silica surface are not in contact and in contact, respectively.

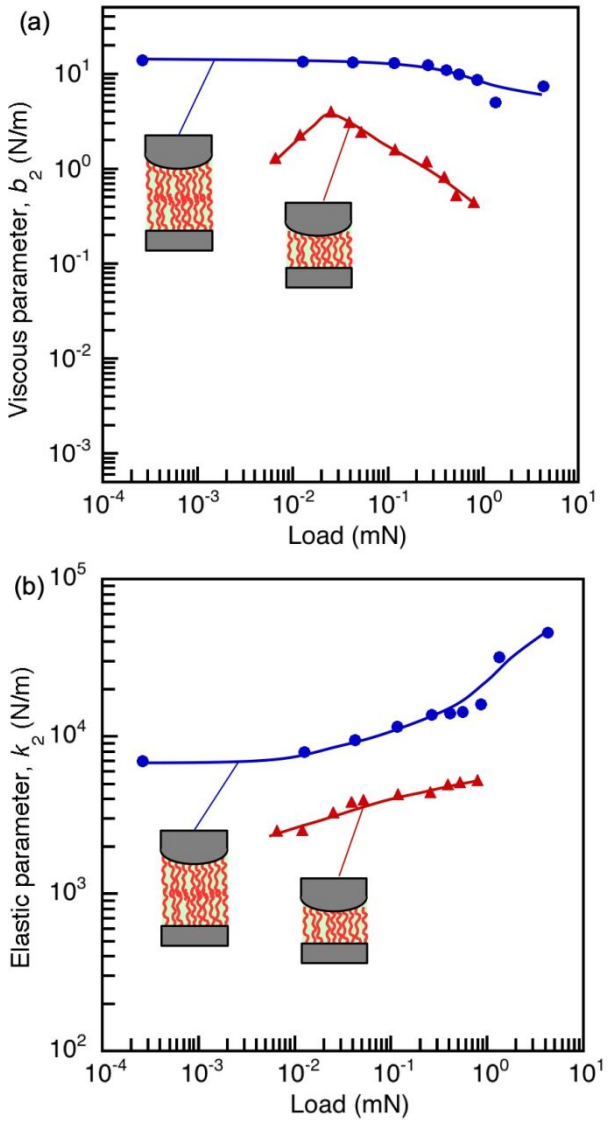

Fig. 9 (a) Plots of elastic (k_2) parameters vs load (L) obtained for the PMMA-PMMA brush layers (blue filled circle) as well as for the PMMA brush-silica (red filled triangle). (b) Plots of viscous (b_2) parameters vs load (L) obtained for PMMA-PMMA brush layers (blue filled circle) as well as for PMMA brush-silica (red filled triangle).

3.5 Shear Amplitude Dependence of PMMA-PMMA Brush Layers.

We showed that the significant increase in the friction between the PMMA-PMMA brush layers by applying an oscillating shear and normal load is due to the interpenetration of the polymer chains. In order to know how the shear motion can affect the interpenetration of the polymer chains, we performed the resonance shear measurement of the PMMA-PMMA brush layers at high shear amplitudes and velocities using the higher input voltage to the piezo tube. Fig. 10 shows the resonance shear curves between the PMMA-PMMA brush layers in toluene measured for various input voltages (U_{in}) at the normal loads of 0.85, 1.34 and 4.28 mN. At the normal load of 0.85 mN (D = 963 nm), a resonance curve was measured at the input voltage U_{in} =1–20 V. With the increasing U_{in}, the normalized amplitude and the frequency of the resonance peak significantly decreased (Fig. 10 (a)). These changes in the resonance curves indicated that the friction between the PMMA-PMMA brush layers decreased with the increasing U_{in}, most probably due to the pulling out of the interpenetrated polymer chains under the high shear amplitude. A similar tendency was observed at the normal loads of 1.34 mN (D = 726 nm) and 4.28 mN (D = 477 nm) with the increasing U_{in} (1 – 50 V) (see Fig. 10 (b), (c)). With the increasing applied load, the resonance amplitude remained higher indicting more interpenetration of the opposed brush chains at the higher applied loads.

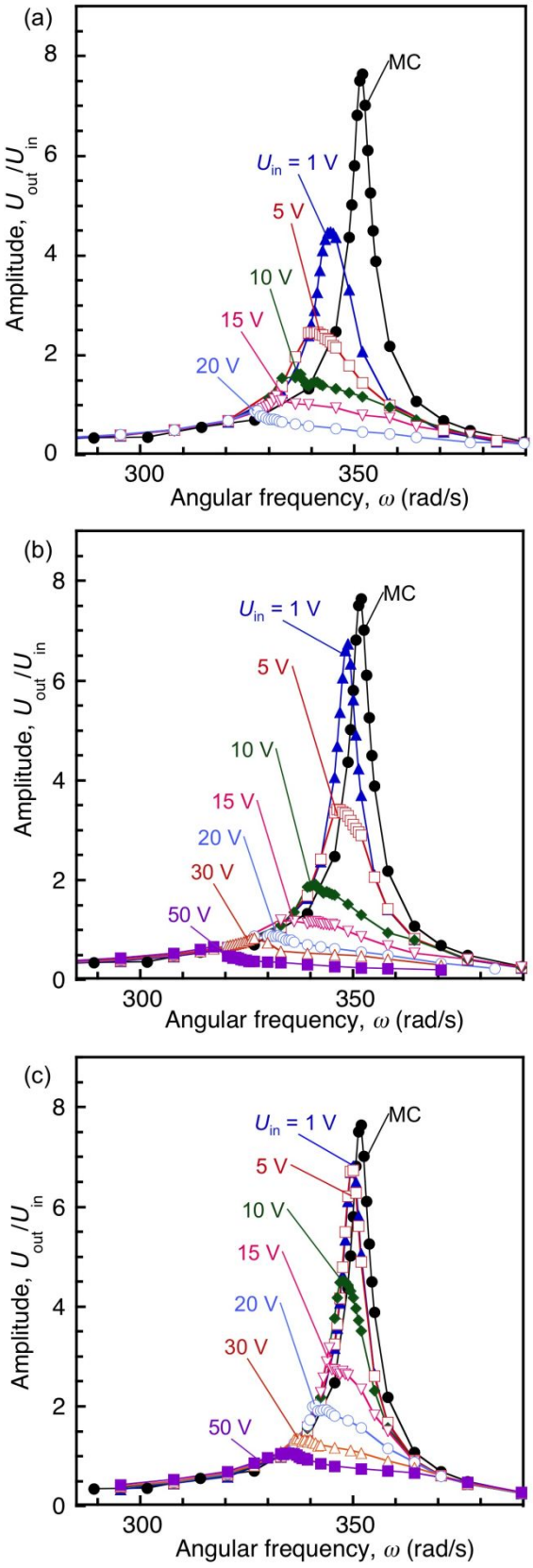
(a)
MC
U_{in} = 1 V
5 V
10 V
15 V
20 V
Amplitude, U_{out}/U_{in}
Angular frequency, ω (rad/s)
(b)
MC
U_{in} = 1 V
5 V
10 V
15 V
20 V
30 V
50 V
Amplitude, U_{out}/U_{in}
Angular frequency, ω (rad/s)
(c)
MC
U_{in} = 1 V
5 V
10 V
15 V
20 V
30 V
50 V
Amplitude, U_{out}/U_{in}
Angular frequency, ω (rad/s)

Fig. 10 Resonance shear curves for the PMMA-PMMA brush layers measured in toluene at various piezo input voltages of 1–50 V. (a) The curves were measured in the load range of 0.85 – 0.82 mN (D = 992 – 762 nm). By applying a higher input voltage U_{in}, the surface separation distance (D) decreased, and as a result, the load also decreased. (b) The curves were measure at the loads of 1.34 – 1.30 mN (D = 764 – 516 nm) at the input voltages of U_{in} = 1 – 50 V. (c) The curves were measured at the loads of 4.28 – 4.25 mN (D = 496 – 322 nm) at the input voltages of U_{in} = 1 – 50 V.

In order to quantitatively evaluate the changes in the properties of the PMMA-PMMA brush layers due to the increase in the shear amplitude and velocity, the damping (b_2) and elastic (k_2) parameters were calculated by analyzing the resonance curves. Fig. 11(a) shows the plots of damping (b_2) and elastic (k_2) parameters (top), and the distances before and after shear (bottom) vs the shear amplitudes (A_{shear}) obtained at L = 1.34 mN. Here, the shear amplitudes (A_{shear}) were obtained as the difference between the positions of upper (x_1) and lower (x_2) surfaces ($A_{shear} = |x_1 - x_2|$) following the previously reported procedure (see Experimental)[28,29] The elastic parameter (k_2) monotonically decreased with the increasing A_{shear}. On the other hand, the viscous parameter (b_2) once increased and reached the maximum at A_{shear} = ca. 60 nm, then decreased with the increasing A_{shear}. These changes in the k_2 and b_2 values should be related to the changes in the structure and dynamics of the PMMA-PMMA brush layers induced by the increasing shear amplitude. A similar tendency was observed for the results obtained at the normal loads (L) of 0.85 (Fig. S3). Fig. 12 shows the plots of the k_2 and b_2 values obtained at L = 4.28 mN. Both the k_2 and b_2 remained constant at the lower A_{shear} below 70 nm, beyond which the changes were similar to those in Fig. 11. This indicated that the interpenetration of the polymer chains were more significant at the greater L, so the greater A_{shear} was required to induce the changes.

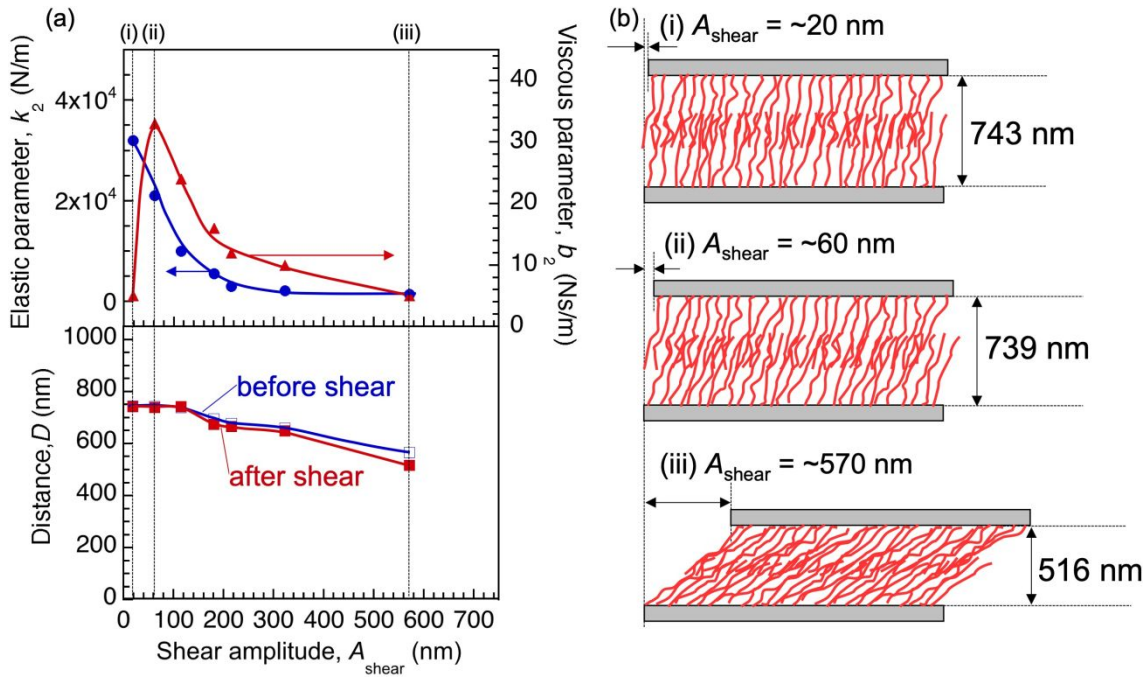

Fig. 11 (a) Plots of the elastic (k_2, filled circle) and damping (b_2, filled triangle) parameters (top), and distance (D) before (open square) and after (filled square) shear measurements (bottom) against the shear amplitude (A_{shear}) obtained at the applied loads of 1.34 mN. (b) Schematic illustration of PMMA brushes drawn based on the results at the shear amplitudes of (i) A_{shear} = 20 nm, (ii) A_{shear} = 60 nm, and (iii) A_{shear} = 570 nm.

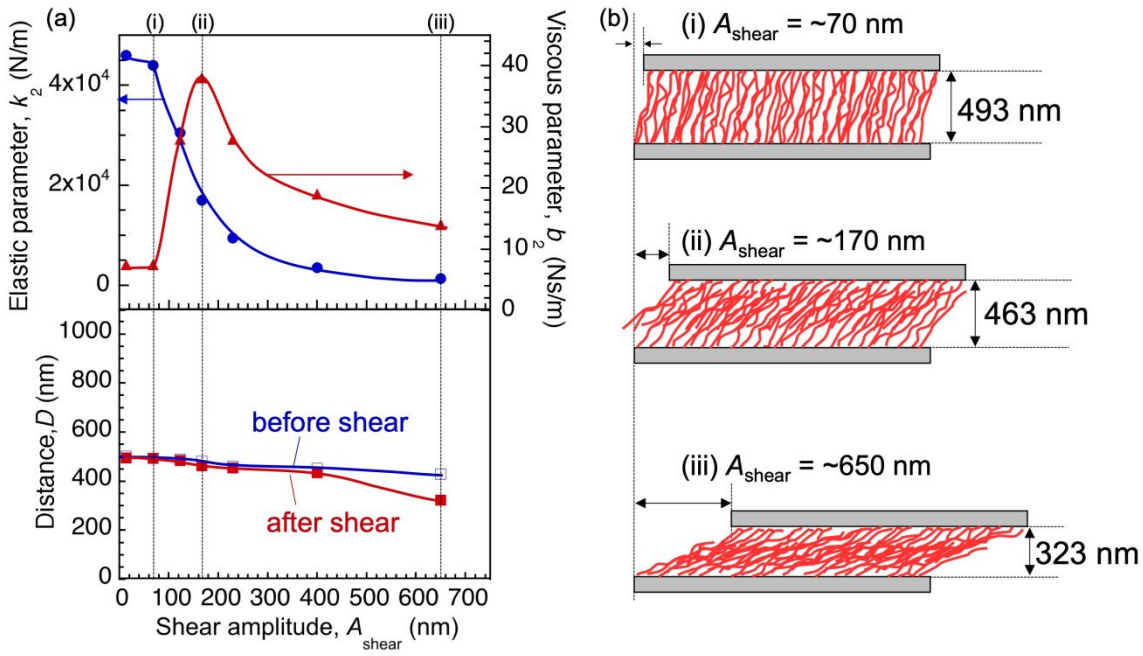

Fig. 12 (a) Plots of the elastic (k_2, filled circle) and damping (b_2, filled triangle) parameters (top), and distance (D) before (open square) and after (filled square) shear measurements (bottom) against the shear amplitude (A_{shear}) obtained at the applied loads of 4.28 mN. (b) Schematic illustration of PMMA brushes drawn based on the results at the shear amplitudes of (i) A_{shear} = 70 nm, (ii) A_{shear} = 170 nm, and (iii) A_{shear} = 650 nm.

3.6 Structure and Dynamics of PMMA Brushes.

Here, we discuss how the structure and dynamics of PMMA brush layers changed under the shear. Our data in Fig. 8 and Fig. 9 indicated that, the polymer chains should be interpenetrated and entangled by applying both the oscillating shear and the normal loads. At A_{shear} = ca. 20 nm and L = 1.34 mN, the brush exhibited highest k_2 and low b_2 values and the surface separation distance (D) showed no change before and after the shear (see Fig. 11-(i)). No change in D under the shear indicated that the interpenetrated and entangled polymer chains did not show significant structure change. The low b_2 value meant that the mobility between the polymer chains as well

as between toluene molecules were suppressed. Therefore, the highest k_2 indicated the deformation/bending of polymer chains should be mainly considered under the applied shear motion. At the A_{shear} of ca. 60 nm (11 % of PMMA layer thickness, see Fig. 11-(ii)), the k_2 value decreased and the b_2 value increased, and the D value showed no change. The decrease in the k_2 value indicated the decrease in the contribution of the deformation/bending of the polymer chains due to the pulling out of the interpenetrated polymer chains. The increase in b_2 indicated that the pulling out of the interpenetrated polymer chains accompanied the increased mobility of polymer chains. With the further increasing A_{shear} above ca. 60 nm, the k_2, b_2 values decreased, and the D value showed the decrease after the shear. This indicated that the interpenetrated polymer chains were further pulled out, thus the energy dissipation (b_2 term) was reduced due to less interactions between the polymer chains. At the A_{shear} above ca. 215 nm (ca. 40 % of PMMA layer thickness, see Fig. 11-(iii)), the decrease in the k_2, b_2 and D values became gradual. This indicated the most part of polymer chains were pulled out by applying the shear amplitudes greater than ca. 40 % of brush layer thickness.

As a reference sample for the without interpenetration case, the PMMA brush-silica system was compared. The k_2, b_2 and D values were obtained and plotted as a function of the A_{shear} at L = 0.79 mN in Fig. S4. Both k_2 and b_2 values were significantly smaller than those obtained for the PMMA-PMMA brushes, and showed no significant change depending on the A_{shear}. This result supported our discussion that the changes in the k_2, b_2 and D values of the PMMA-PMMA brush layers were due to changes in structures and dynamics of the entangled polymer chains of the opposed brush layers.

The A_{shear} dependencies of k_2, b_2, and D values obtained at L = 0.85 mN (Fig. S3) were similar to those at L = 1.34 mN (Fig. 11), while the b_2 and k_2 values at L = 0.85 mN were smaller than

those at L = 1.34 mN indicating much less interpenetration at L = 0.85 mN. At L = 4.28 mN (Fig. 12), the b_2, k_2 values showed no change at the A_{shear} less than ca. 70 nm, while they significantly changed at A_{shear} < ca. 60 nm at L = 1.34 mN. This indicated that the interpenetration of PMMA chains was more significant at L = 4.28 mN, and the greater shear amplitudes were required to pull out the interpenetrated PMMA chains.

For the PMMA brush-silica, the b_2 parameter drastically increased after contact (Fig. 8(a)), then decreased with the increasing load (at L > 0.025 mN) (Fig. 9(a)), while the k_2 parameter for the PMMA brush-silica monotonically increased with the increasing load (Fig. 9(b)). For the PMMA brush-silica, the PMMA chains directly interacted with the opposed silica surface as the surfaces approached, thus the b_2 damping parameter could increase in the low load range ($L \leqq$ 0.03 mN). The attractive interaction between the PMMA brush and the silica surface was confirmed by the adhesion force of ca. 2 mN/m observed on separation of PMMA brush-silica surfaces (Fig. S5). The structure of the PMMA chains should have transformed into a more compact structure with the increasing normal load. This resulted in the reduced b_2 damping parameter (energy dissipation) and the monotonically increase in the elastic k_2 value.

The friction force ($F_{friction}$) was obtained using the damping (b_2) and elastic (k_2) parameters as well as the shear amplitude (A_{shear}) and velocity (V_{shear}) using the equation, $F_{friction} = \max|b_2 \times V_{shear} + k_2 \times A_{shear}|$.[28] The $F_{friction}$ value obtained at the A_{shear} of ca. 20 nm was 0.589 mN, and the contribution of elastic term ($k_2 \times A_{shear}$) to the total $F_{friction}$ was more than 99%. The $F_{friction}$ value obtained at the A_{shear} of ca. 60 nm was 1.486 mN, and the contribution of elastic term ($k_2 \times A_{shear}$) to the total $F_{friction}$ decreased to 77%. The $F_{friction}$ value obtained at the A_{shear} of ca. 570 nm was 1.167 mN, and the contribution of elastic term ($k_2 \times A_{shear}$) to the total $F_{friction}$ further decreased to 47%. The friction coefficient values obtained at L = 0.85, 1.34 and 4.28 mN were at the order of

10^{-1}. This was greater than the typical friction coefficient of CPBs as low as 10^{-3} obtained by AFM,[15,16] though the friction coefficient of the current study varied within the range of 0.1–1.0 in a complex manner depending on the condition such as the elastic and viscous parameters, and the sliding amplitude and velocity. One significant difference between the colloidal probe AFM (CP-AFM) and the RSM is the size of the surfaces, i.e., the CP-AFM uses a colloidal sphere (radius = 5 μm) and a flat surface geometry, and the RSM uses a crossed cylinder (radius = 2 cm) geometry. Based on the surface forces profiles (Fig. 4), the contact pressures for RSM and CP-AFM were estimated, and the friction coefficients obtained by RSM and CP-AFM were compared at the similar contact pressure.[37] In the CP-AFM on PMMA brushes, the friction coefficient below 10^{-3} was obtained up to the contact pressure of 0.039 MPa, which corresponded to the normal load of 30 nN.[15] On the other hand, in the RSM on PMMA brushes, a quite high friction coefficient of ca. 1 was obtained at the similar contact pressure of 0.084 MPa, which corresponded to the D = 970 nm, L = 0.85 mN (Fig.5). Thus, the difference between the surface sizes of the CP-AFM and the RSM could not explain the high friction obtained in the RSM. Another possible reason for the high friction coefficients obtained in this study could be the application of an oscillating shear motion, while the sliding of the constant velocity was applied during the AFM. Besides the oscillatory shear motion, the relatively small shear amplitude compared with the diameter of the contact area in the RSM could be a reason of the high friction coefficient remained within the shear amplitude range used in this study. In order to reduce the friction in these conditions, employment of the polymer brush with cyclic structures[19] or asymmetric polymer brushes layers which are immiscible[20] should be efficient. Thus, the obtained results indicated the importance of the operating conditions of the CPBs for tribological application, and the possibility of the friction control by tuning of the shear condition as well as chemical structures of polymers.

4 Conclusion

In this study, we employed surface forces and resonance shear measurements (RSM) for studying the structure and properties of concentrated polymer brushes (CPB) of poly(methylmethacrylate) (PMMA) swollen in toluene.

(i) During the surface forces measurement, the steric repulsive forces were observed due to the contact and the compression of the opposed PMMA brush layers. The force profiles showed clear hysteresis between the compression and decompression processes. However, no adhesion force was observed between the PMMA brush layers in toluene after compression of the layers. This means that entanglement of the polymer chains occurred only within a PMMA brush layer and no interpenetration was induced by the normal compression.

(ii) Based on the resonance shear measurement, the damping (b_2) and elastic (k_2) parameters were obtained for the PMMA-PMMA brushes as well as for the PMMA brush-silica by analyzing the resonance curves. For the PMMA-PMMA brush layers, both the damping b_2 and elastic k_2 parameter drastically increased after the contact of the opposed PMMA brush layers. The b_2 parameter slightly decreased and the k_2 parameter monotonically increased with the increasing normal load. As references, the b_2 and k_2 parameters were obtained for the PMMA brush-silica, and exhibited similar load dependencies. However, both the b_2 and k_2 values for the PMMA-PMMA brushes were significantly higher than those obtained using the PMMA brush-silica for the whole range of the applied normal load. This indicated that the interpenetration of the polymer chains for the PMMA-PMMA brush layers occurred by applying the oscillating shear and the normal load.

(iii) For the PMMA-PMMA brushes under the normal loads (L) of 0.84, 1.34 and 4.28 mN, the effects of the high shear amplitudes (A_{shear}) on the properties and the structure of the PMMA brush

were investigated. With the increasing shear amplitude on the compressed PMMA brushes, the damping parameter (b_2) once increased, reached a maximum, then decreased, while the elastic parameter (k_2) monotonically decreased. At the lowest shear amplitude (A_{shear} = ca.20 nm), the polymer chains had interpenetrated and entangled, thus the deformation/bending of the polymer chains should be mainly considered under the applied shear motion. This could explain the high k_2 and the low b_2 values at the lowest shear amplitude. The decrease in the k_2 value indicated that the interpenetrated polymer chains were gradually pulled out. The increase in b_2 (energy dissipation) may be due to the greater mobility of the terminal groups of the polymer chains during the pulling out of the interpenetrated polymer chains. The decrease in both the b_2 and k_2 values at the greater shear amplitudes indicated that the polymer chains were further pulled out, and the energy dissipation was reduced. Our results indicated that at L = 1.34 mN, the most part of polymer chains were pulled out by applying the shear amplitudes greater than ca. 40 % of swollen brush layer thickness. At L = 4.28 mN, the interpenetration of PMMA chains became more significant, and the greater shear amplitudes were required to pull out the interpenetrated PMMA chains.

Our study of the PMMA brushes based on the surface forces and resonance shear measurements provided new insights into how the structure of the PMMA brushes changed under the load and the oscillating shear, and how it regulates their properties, friction and lubrication. One of the most expected applications of the CPBs is an artificial articular cartilage, which moves in a reciprocal way with a relatively long stationary state. Industrial mechanical products such as sealing parts for piston, sliding parts in speaker also moves in a reciprocal way or vibrates at various frequencies. Our study indicates that it is important to consider the structure and/or the sliding motions in order to maintain low friction. In another words, the results suggest a potential

to control the friction (traction) or adhesion forces of the CPBs by tuning the shear conditions or the application of the external mechanical stimulus.

Conflicts of interest

There are no conflicts to declare.

Acknowledgments

This study was supported by the “Accelerated Innovation Research Initiative Turning Top Science and Ideas into High-Impact Values (ACCEL)” of the Japan Science and Technology Agency (JST), and “Research and Development of Next-Generation Filed” from the Ministry of Education, Culture, Sports, Science and Technology, Japan.

Notes and References

1. G. J. Fleer, M. A. Cohen-Stuart, J. M. H. M. Scheutjens, T. Cosgrove and B. Vincent, *Polymes at Interfaces*, Chapman and Hall, London, 1993.
2. D. H. Napper, *Polymeric stabilization of colloidal dispersions*, Academic Press, London, 1983.
3. L. H. Lee, *Fundamentals of Adhesion*, Plenum, New York, 1991.
4. J. A. Koehler, M. Ulnricht and G. Belfort, *Langmuir*, 1997, **13**, 4162.
5. U. Raviv, R. Tadmor and J. Klein, *J. Phys. Chem. B*, 2001, **105**, 8125–8134.
6. U. Raviv, S. Giasson, N. Kampf, J.-F. Gohy, R. Jéröme and J. Klein, *Nature*, 2003, **425**.
7. M. T. Müller, X. Yan, S. Lee, S. S. Perry and N. D. Spencer, *Macromolecules*, 2005, **38**, 5706-5713.
8. M. Chen, W. H. Briscoe, S. P. Armes and J. Klein, *Science*, 2009, **323**, 1698-1701.
9. M. Ejaz, S. Yamamoto, K. Ohno, Y. Tsujii and T. Fukuda, *Macromolecules*, 1998, **31**, 5394.
10. M. Husseman, E. E. Malmstrom, M. McNamara, M. Mate, D. Mecerreyes, D. G. Nenoit, J. L. Hedrick, P. Mansky, E. Huang, T. P. Russell and C. J. Hawker, *Macromolecules*, 1999, **32**, 1424.
11. B. Zhao and W. J. Brittain, *J. Am. Chem. Soc.*, 1999, **121**, 3557.
12. S. Yamamoto, M. Ejaz, Y. Tsujii and T. Fukuda, *Macromolecules*, 2000, **33**, 5608-5612.
13. S. Yamamoto, M. Ejaz, Y. Tsujii, M. Matsumoto and T. Fukuda, *Macromolecules*, 2000, **33**, 5602-5607.
14. Y. Tsujii, K. Ohno, S. Yamamoto, A. Goto and T. Fukuda, *Adv. Polym. Sci.*, 2006, **197**, 1-45.
15. Y. Tsujii, A. Nomura, K. Okayasu, W. Gao, K. Ohno and T. Fukuda, *J. Phys.: Conf. Ser.*, 2009, **184**, 012031.
16. A. Nomura, K. Okayasu, K. Ohno, T. Fukuda and Y. Tsujii, *Macromolecules*, 2011, **44**, 5013-5019.

17. T. Kreer, *Soft Matter*, 2016, **12**, 3479-3501.
18. N. Iuster, O. Tairy, M. J. Driver, S. P. Armes and J. Klein, *Macromolecules*, 2017, **50**, 7361-7371.
19. M. Divandari, L. Trachsel, W. Yan, J.-G. Rosenboom, N. D. Spencer, M. Zenobi-Wong, G. Morgese, S. N. Ramakrishna and E. M. Benetti, *ACS Macro Lett.*, 2018, **7**, 1455-1460.
20. S. d. Beer, E. Kutnyanszky, P. M. Schön, G. J. Vancso and M. H. Müser, *Nat. Commun.*, 2014, **5**, 3781.
21. M. Ejaz, S. Yamamoto, K. Ohno, Y. Tsujii and T. Fukuda, *Macromolecules*, 1998, **31**, 5934-5936.
22. H.-Y. Ren, M. Mizukami and K. Kurihara, *Rev. Sci. Instrum.*, 2017, in press.
23. K. Ohno, T. Morinaga, K. Koh, Y. Tsujii and T. Fukuda, *Macromolecules*, 2005, **38**, 2137-2142.
24. T. Morinaga, M. Ohkura, K. Ohno, Y. Tsujii and T. Fukuda, *Macromolecules*, 2007, **40**, 1159-1164.
25. W. Wunderlich, in *Polymer Handbook*, eds. J. Brandrup, E. H. Immergut and E. A. Grulke, John Wily & Sons Inc, New York, 4th edition edn., 1999, pp. 87-90.
26. J. N. Israelachvili, *J. Colloid Interface Sci.*, 1973, **44**, 259-272.
27. J. N. Israelachvili, *Intermolecular and Surface Forces*, 3rd edn., Academic Press, Ltd., New York, 2010.
28. M. Mizukami, S. Hemette and K. Kurihara, *Rev. Sci. Instrum.*, 2019, **90**, 055110.
29. M. Mizukami and K. Kurihara, *Rev. Sci. Instrum.*, 2008, **79**, 113705.
30. W.-P. Liao, I. G. Elliott, R. Faller and T. L. Kuhl, *Soft Matter*, 2013, **9**, 5753-5761.
31. J. Watanabe, M. Mizukami and K. Kurihara, *Tribol. Lett.*, 2014, **56**, 501-508.
32. J. D. Ferry, *Viscoelastic Properties of Polymers, 3rd Edition*, 3rd edn., Wiley & Sons, New York, 1980.
33. M. Mizukami, K. Kusakabe and K. Kurihara, *Prog. Colloid Polym. Sci.*, 2004, **128**, 105-108.
34. H. Sakuma, K. Otsuki and K. Kurihara, *Phys. Rev. Lett.*, 2006, **96**, 046104.
35. K. Ueno, M. Kasuya, M. Watanabe, M. Mizukami and K. Kurihara, *Phys. Chem. Chem. Phys.*, 2010, **12**, 4066-4071.

36. T. Kamijo, H. Arafune, T. Morinaga, S. Honnma, T. Sato, M. Hino, M. Mizukami and K. Kurihara, *Langmuir*, 2015, **31**, 13265-13270.

37. The contact area of the opposed PMMA brush layers at the distances below the onset of the repulsion was calculated using the normal force profile shown in Fig. 4 (2nd approach). By applying the scaling law for the PMMA brush thickness, the contact pressure at the normal load of 30 nN applied in the case of CP-AFM,[15] was estimated to be 0.039 MPa at which the friction coefficient of 10^{-3} was obtained. On the other hand, at the similar contact pressure of 0.084 MPa (the smallest applied pressure for a systematic study) in the RSM, corresponded to the D = 970 nm, L = 0.85 mN (Fig.5), a quite high friction coefficient of ca. 1 was obtained.

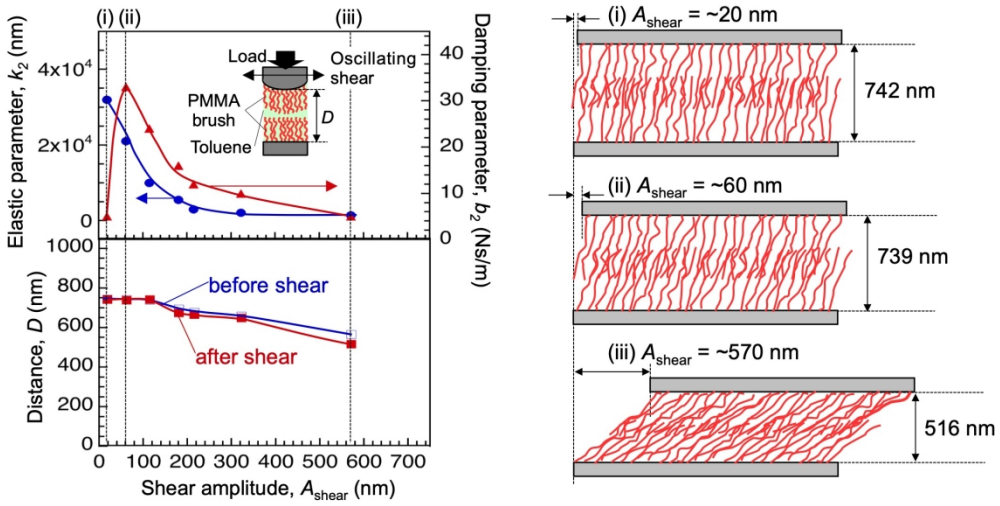

758x386mm (72 x 72 DPI)